Assessing the Potential of NH_3/H_2-Fueled Gas Turbines for Carbon Free Power Generation: A Comprehensive Analysis of Operating Behavior and Performance

Valentina Veltroni[a], Viola Masi[b], Carlo Carcasci[c]

[a] *University of Florence, Department of Industrial Engineering (DIEF), Florence, Italy, valentina.veltroni@unifi.it*

[b] *University of Florence, Department of Industrial Engineering (DIEF), Florence, Italy, viola.masi@unifi.it*

[c] *University of Florence, Department of Industrial Engineering (DIEF), Florence, Italy, carlo.carcasci@unifi.it*

Abstract:

The transition toward carbon-free power generation is driving interest in chemical energy carriers for storing renewable electricity. Hydrogen is widely studied for this purpose, but its storage costs and infrastructure constraints motivate alternative solutions. Converting hydrogen into ammonia offers advantages in terms of storage costs, handling, and compatibility with existing transport and storage infrastructure. Within this context, the use of green ammonia as a sustainable fuel in gas turbines has gained increasing attention. In practical applications, partial ammonia cracking is often employed to enhance fuel reactivity, leading to NH_3/H_2 mixtures. Both pure ammonia and ammonia/hydrogen fuels, however, pose challenges related to NO_X emissions and ammonia slip, requiring redesigned combustors for retrofitting existing gas turbine systems.

This work investigates NH_3/H_2-fueled gas turbine operation through a coupled modelling framework that integrates a system-level gas turbine model with a chemical reactor network, ensuring a consistent representation of turbomachinery behavior and combustion chemistry. The turbomachinery layout is derived from a methane-fired reference gas turbine and retained for off-design NH_3/H_2 operation, while the combustor is redesigned using a rich–quench–lean configuration and modelled through a network of perfectly stirred and plug-flow reactors, capturing finite-rate chemistry, NO_X formation, and unburned ammonia.

By linking fuel chemistry and turbomachinery constraints under off-design conditions, the results show how variations in fuel blend affect NO_X emissions and overall performance in the retrofit of the reference turbine to NH_3/H_2 operation, enabling identification of suitable design combustion parameters, such as rich-zone equivalence ratio and fuel composition, that provide the best compromise between emissions and cycle performances.

Overall, the proposed framework provides a consistent tool to assess NH_3/H_2 gas turbine operation and supports combustor design and retrofitting strategies.

Keywords:

Hydrogen/ammonia fuels; Gas turbines; Chemical Reactor Network; NO_X emissions

1. Introduction

The need to mitigate CO_2 emissions is accelerating the transition toward low-carbon energy systems. In power generation, this shift involves both large-scale deployment of renewables and technologies to reduce emissions from existing plants. Gas turbines are widely used for their flexibility, rapid start-up, high power-to-weight ratio and relatively low emissions, yet natural gas operation still produces significant CO_2. This drives growing interest in carbon-free fuels for gas turbines, through co-firing or full fuel substitution.

Among the possible alternatives, green hydrogen produced from renewable electricity through water electrolysis, is considered one of the most promising carbon-free fuels for power generation. Hydrogen can be used in gas turbines with relatively limited modifications, allowing partial or complete decarbonization of existing plants while preserving their operational flexibility, which is essential for balancing the variability of renewable energy sources. Despite these advantages, hydrogen presents significant challenges related to transportation and storage due to its low volumetric energy density. For this reason, alternative hydrogen carriers are receiving increasing attention. Among them, ammonia is particularly attractive because it does not contain carbon, has a relatively high volumetric energy density, and benefits from an already established

infrastructure for transport and storage. Moreover, it can be used directly in gas turbines. However, ammonia combustion poses challenges, including high ignition temperature, low laminar burning velocity, and slow chemical kinetics [1]. Under ideal conditions ammonia combustion proceeds according to the global reaction:

$$4\mathrm{NH_3} + 3\mathrm{O_2} \rightarrow 2\mathrm{N_2} + 6\mathrm{H_2O} \quad (1)$$

In real combustion environments several reaction pathways contribute to NO_X formation. Because ammonia contains nitrogen in its molecular structure, fuel-bound nitrogen becomes an additional source of NO_X emissions, in addition to the conventional thermal formation mechanisms. As a result, ammonia combustion typically produces higher NO_X levels than conventional hydrocarbon fuels [1,2]. To address these issues, several strategies have been proposed to improve ammonia combustion in gas turbines. Hydrogen blending is one of the most widely investigated approaches, as it increases laminar burning velocity and enhances mixture reactivity. It also promotes the formation of reactive radicals (H, O, OH), accelerating ammonia oxidation and enabling combustion at lower temperatures [2]. Staged combustion, particularly in rich-quench-lean configurations, is widely adopted to control NO_X emissions while maintaining high combustion efficiency [3]. In addition, post-combustion technologies such as selective catalytic reduction can further reduce NO_X emissions by converting them into N_2 in the exhaust stream [3].

1.1. Scope of the work

Despite the growing interest in ammonia and ammonia/hydrogen fuels for gas turbine applications, significant challenges remain in predicting their combustion behavior within practical combustor configurations and assessing their impact on overall gas turbine performance. In particular, the strong coupling between combustion chemistry and gas turbine cycle operation requires the integration of detailed chemical kinetic analysis with system-level modeling approaches. In this context, the present work investigates the combustion behavior of ammonia/hydrogen mixtures in a gas turbine combustor through a Chemical Reactor Network (CRN) model coupled with a gas turbine cycle simulation tool. The objective of this study is to assess the feasibility of retrofitting an existing methane-fired gas turbine to operate with ammonia/hydrogen fuel mixtures, assuming fixed turbomachinery geometry and changing combustor design. The analysis focuses on how the fuel change affects emissions, overall cycle performance, and the resulting off-design operation of the turbomachinery.

2. Modeling approach

This work combines a modular gas turbine cycle simulation code, able to represent turbomachinery in detail and solve the cycle, with a CRN combustion model. The cycle model performs both design and off-design analyses, defining turbomachinery operating conditions and their response to changes in fuel composition and control settings. The CRN model provides information on the combustion products. The two models are coupled through an iterative exchange of boundary conditions.

2.1. Gas Turbine Cycle Model

The simulations of the gas turbine cycle were carried out using the ESMS modular code. A detailed description of the code and its theoretical background can be found in previous studies [4–6]. New plant layouts can be defined by connecting a set of elementary components that represent individual unit operations, such as compressors, turbines, mixers, and heat exchangers. Each component is modeled as a black box that simulates a specific thermodynamic transformation. In this work, combustor chemistry is evaluated externally, and the resulting exhaust mass flow rate and composition are provided to the ESMS code, which performs the system simulation with the updated working fluid. The complete plant model is described by a set of nonlinear equations. During the solution process, these equations are linearized, while the coefficients are updated iteratively during the calculation. The resulting system is solved simultaneously using a matrix-based method, following a fully implicit linear approach. The code supports both design and off-design simulations. During the design phase, the geometry and the main operating parameters of the compressor and turbines are determined. These include quantities such as compressor and turbine velocity triangles at the mean radius and cascade parameters. Once the design configuration is established, off-design analyses can be performed by imposing new boundary conditions.

2.2. Chemical Reactor Network Combustor Model

CRN models have been widely adopted for kinetic studies in gas turbine combustors, even for NH_3/H_2 mixtures [7–11], since they allow rapid evaluation of pollutant emissions and combustion behavior while retaining detailed chemical kinetics. The CRN method solves simplified transport equations to represent combustion processes through idealized reactors, mainly Perfectly Stirred Reactors (PSR) and Plug Flow Reactors (PFR). These interconnected reactors exchange mass and heat, creating a network designed to retain the essential characteristics of the overall flow field. The PFR model assumes that the fluid flows through the reactor without axial diffusion, effectively moving as plug-like elements. The PSR model instead assumes perfectly homogeneous and instantaneous mixing between reactants and products. In practical combustor representations, PSR models are typically used for the primary (flame or ignition) zone, where strong recirculation promotes intense mixing, while PFR models are used to describe combustion and transport in the intermediate and dilution zones. The CRN simulations were performed using the open-source package Cantera [12].

For the baseline methane-fueled gas turbine, a CRN representing a Dry Low NOx (DLN) combustor was implemented following the approach reported in [13], consistent with the annular DLE combustion chamber of the reference gas turbine simulated. The primary zone is modeled with a single PSR continuously fed with premixed air and methane. The combustion products leaving the PSR are then mixed with dilution air before entering the intermediate zone, which is modeled with a PFR. The products leaving the first PFR are again diluted with additional air before entering the dilution–cooling zone, represented by a second PFR. The reactor network was implemented using the same input conditions reported in [13], including pressure, inlet temperature of air and fuel, air and fuel mass flow rates, fuel composition, and reactor volumes. Through an iterative procedure, the equivalence ratios of the different zones were adjusted to reproduce the temperature profile reported in the reference study. The resulting equivalence ratios for the primary and intermediate zones, together with the residence times of the reactors, were then used for the simulations of the gas turbine considered in this work, while the global equivalence ratio was determined by the required Turbine Inlet Temperature (TIT). The GRI-Mech 3.0 kinetic mechanism [14] was adopted for methane combustion.

For the retrofitting of the combustor to operate with hydrogen and ammonia, a two-stage Rich-burn/Quick-mix/Lean-burn (RQL) configuration was investigated. This concept is widely considered one of the most effective solutions that show promise for good stability and low NO_X emissions [8–10,15,16] for NH_3/H_2 fuels. In the rich-burn stage, NO_X formation is suppressed under fuel-rich conditions, while the remaining fuel is oxidized in the subsequent lean stage after rapid mixing with secondary air. The CRN model for the RQL combustor was developed following the configuration reported in [8,9,16]. Each stage of the combustor is represented by a PSR followed by a PFR. Upstream of the rich stage, a premixed air–fuel mixture is specified. The outlet state of the rich stage is then fed to the lean stage together with an injection of secondary air. The mass flow rate of the secondary air was determined to achieve a target global equivalence ratio. The residence time was specified for each element of the network following values reported in [8]. Since Cantera does not allow the residence time of a PSR to be set directly, the reactor volume was iteratively adjusted for a fixed total mass flow rate until the desired residence time was obtained. The equivalence ratio in the rich stage ϕ_r was varied between 1.1 and 1.5, while the global equivalence ratio ϕ_g was determined as for the DLN combustor by the required TIT. As discussed in [16], NO_X formation in the low-NO_X operating regime is more sensitive to ϕ_r than to ϕ_g. This allows the combustor outlet temperature, and therefore the TIT, to be adjusted by varying the amount of secondary air without significantly increasing NO_X emissions. The chemical kinetics of the ammonia/hydrogen mixture were described using the Okafor mechanism [17], which was selected to ensure accurate prediction of combustion and emission characteristics under elevated pressure conditions [7]. This mechanism was also chosen because it provides a conservative prediction of NO_X formation among the mechanisms evaluated in [8].

The CRN architecture of the two combustors is shown in Figure 1.

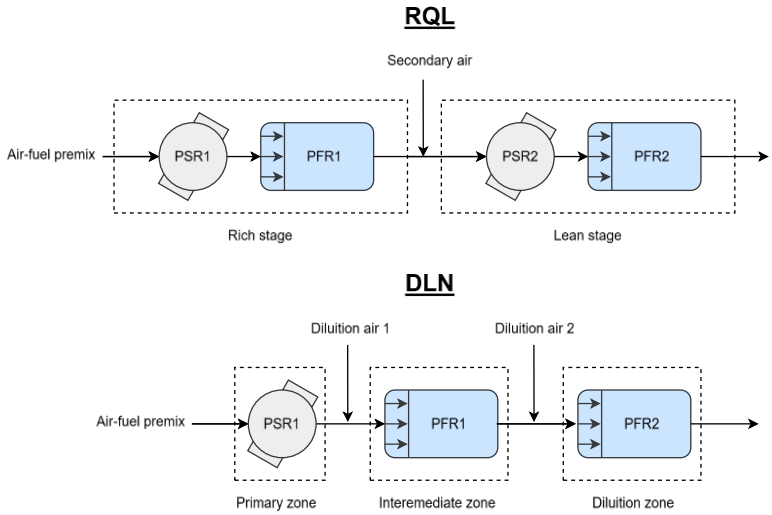

Figure 1: *Two-stage RQL combustion model (H_2/NH_3) and DLN combustion model (CH_4) using PSR-PFR CRN.*

The results from the RQL CRN model were compared to published data from [8] showing good agreement, as visible in Figure 2. The model was run under the same conditions reported in [8], which included pure NH_3 combustion, a pressure of 12 atm, reactant preheating to 600 K, rich stage PSR and PFR residence times of 3 ms and 14 ms, respectively, and lean stage PSR and PFR residence times of 2 ms and 1 ms, respectively.

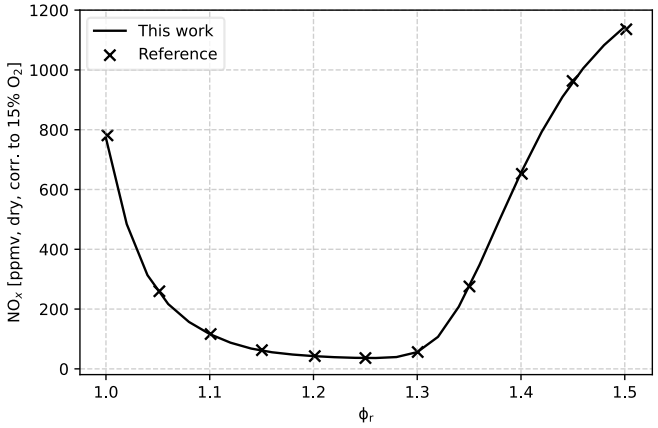

Figure 2: *Cantera two-stage PSR-PFR CRN NO_X (15% O_2 dry) results, along with Chemkin results from Li et al. [8], for pure NH_3 combustion, 600 K preheat, 12 atm (Okafor mechanism).*

The CRN model was developed in Python using Cantera and coupled with the ESMS code. The coupled calculation starts with an initial ESMS simulation using a first estimate of the combustion products composition and fuel mass flow rate. The resulting values of air mass flow rate, temperature, and pressure at the combustor inlet are then used as input for the CRN model. The TIT, determined within the cycle model in ESMS according to the imposed operating conditions, is enforced in the CRN by adjusting the global equivalence ratio, while the equivalence ratio in the rich zone is imposed as an input parameter. The CRN model computes the combustion process and the resulting composition and mass flow rate of the combustion products. The combustion products calculated by the CRN are returned to ESMS, and the iterative exchange between the two models continues until convergence is achieved. The pressure drop is applied only at the combustor outlet as an input parameter in ESMS. The combustion model also performs the combustor sizing based on the imposed residence times.

3. Results and Discussion

3.1. Baseline Methane-Fired Gas Turbine

This section describes the design-point modeling of the reference gas turbine operating with methane. Starting from this baseline configuration, the fuel was replaced with hydrogen/ammonia mixtures. The resulting

variations in fuel properties and mass flow rate shift the operating conditions of the gas turbine, making off-design analysis necessary to capture the response of the turbomachinery.

The gas turbine considered in this study is a two-shaft machine based on the LT16 turbine by Baker Hughes [18], a 16 MW class unit. The main design parameters of the system are reported in Table 1. The gas turbine model was calibrated using the design-point data provided by the manufacturer. Since only a limited set of parameters is publicly available, several assumptions were required to complete the model. The operating conditions and design parameters available from the manufacturer, including compressor pressure ratio, inlet ISO conditions, low-pressure turbine rotational speed, exhaust temperature and pressure, and the number of turbomachinery stages, were imposed in the model. The inlet air mass flow rate and net efficiency were not imposed and were instead used as calibration targets. The turbomachinery design parameters required by the mean-line model, namely the flow coefficient, loading coefficient, and degree of reaction, were derived from literature for industrial gas turbines [19,20]. The combustion chamber was simulated through the CRN representing a DLN combustor as reported in Section 2.2. Several parameters that are not disclosed by the manufacturer, such as the isentropic efficiencies of the compressor and turbines, the combustor pressure drop, and the cooling mass flow rate, were assumed and iteratively adjusted until the calculated values of air mass flow rate and net efficiency matched the reported data. The gas generator rotational speed was fixed at a typical value reported in the literature for similar two-shaft gas turbines [21]. All the remaining quantities reported in Table 1 were calculated by the model.

***Table 1**: Design parameters and performance data of the reference gas turbine. Manufacturer data were used as imposed conditions when available, except for air mass flow rate and overall efficiency that were used as calibration parameters by comparing model predictions with manufacturer data.*

Component	Parameter	Reference [18]	Simulation	Type of parameter
Compressor	**Inlet air mass flow rate (21% O_2, 79% N_2 vol.)**	**53.30 kg/s**	**53.62 kg/s**	**Calculated (0.58% error)**
	Inlet pressure	101325 Pa	101325 Pa	Input
	Inlet temperature	288.15 K	288.15 K	Input
	Pressure ratio	19.3	19.3	Input
	N° of compressor stages	12	12	Input
	Rotational speed	-	9800 rpm	Assumed input
	Isentropic efficiency	-	91.4%	Assumed input
Combustor	Fuel mass flow rate	-	0.89 kg/s	Calculated
	Pressure loss	-	3.6%	Assumed input
Turbines	Rotational speed LP	7800 rpm	7800 rpm	Input
	Rotational speed HP	-	9800 rpm	Assumed input
	N° of turbine stages	2 (HP) + 2 (LP)	2 (HP) + 2 (LP)	Input
	TIT	-	1499 K	Calculated
	LP turbine exhaust temperature	755.15 K	755.15 K	Input
	LP turbine exhaust pressure	101325 Pa	101325 Pa	Input
	Turbine exhaust mass flow rate	-	54.50 kg/s	Calculated
	HP turbine isentropic efficiency	-	83.79%	Assumed input
	LP turbine isentropic efficiency	-	85.79%	Assumed input
	Coolant mass flow rate	-	10.80 kg/s	Assumed input
Performance	Net power	16.8 MW	16.8 MW	Input
	Net efficiency	**37.30%**	**37.91%**	**Calculated (1.64% error)**

The off-design model was validated by evaluating performance in different ambient conditions. The results confirm that the model reproduces the expected trends of the reference gas turbine [18], as shown by the comparison between the manufacturer performance maps and the model predictions reported in Figure 3.

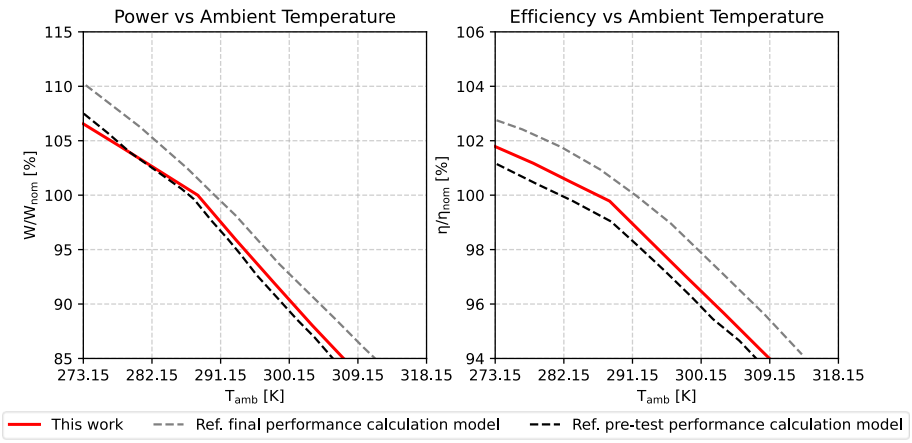

***Figure 3**: Gas turbine output shaft power and shaft efficiency as a function of ambient temperature: comparison between manufacturer data and model predictions.*

3.2. Gas Turbine Retrofitting for NH_3/H_2 Operation

Retrofitting an existing gas turbine from natural gas to hydrogen/ammonia fuels requires modifications to the combustor, while the main turbomachinery can remain unchanged [15]. Since these fuels differ significantly from conventional natural gas, the combustor must be redesigned to ensure stable operation, compliance with emission limits, and proper integration with the existing turbine components. For this reason, the system has to be evaluated as a whole, accounting for both turbine operating conditions and detailed combustion behavior.

All simulations were performed using the same baseline turbine geometry, replacing only the original combustor with the RQL configuration described in Section 2.2 and assuming the same pressure drop. The fuel blend was assumed to be at ambient temperature. Two constraints were imposed to ensure a consistent comparison with the original configuration. First, the rotational speed of the low-pressure turbine was kept constant, since it is mechanically coupled to the generator and therefore fixed by the grid frequency. Second, the turbine was required to deliver the same nominal power, so that the electrical output of the retrofitted configuration matches that of the baseline gas turbine. In addition to this reference condition, an alternative retrofit strategy was also considered: evaluating the maximum power achievable with the new fuel blend. This additional case is analyzed in order to assess how different operating constraints influence the performance of the retrofitted gas turbine.

To understand the differences arising in the gas turbine when changing the fuel, it is useful to consider the main properties of ammonia and hydrogen compared with methane, as well as the differences between the two alternative fuels themselves [3]:

- Lower Heating Value (LHV): methane has an LHV of 50 MJ/kg, ammonia has a significantly lower value of 18.6 MJ/kg, while hydrogen has a much higher LHV of 120 MJ/kg.
- Combustion product composition**:** in hydrogen and ammonia combustion CO_2 is not produced. H_2 combustion ideally produces only water vapor, whereas NH_3 combustion generates mainly N_2 and H_2O. As a result, the composition of the combustion products changes respect to methane combustion, leading to different thermodynamic properties such as the specific heat capacity (c_p), gas constant (R), and heat capacity ratio (γ).
- Air–Fuel Ratios (AFR): the stoichiometric AFR by mass is 17.2 for CH_4, 6.05 for NH_3 and 34.3 for H_2.
- Different flame temperatures. Hydrogen exhibits a high adiabatic flame temperature of ~2500 K, methane shows an intermediate value of ~2220 K, while ammonia has a significantly lower flame temperature (~1850 K).

3.2.1 Fixed Power Retrofitting

The retrofit was first evaluated under the constraints of fixed low pressure spool rotational speed and fixed power output, equal to the nominal value of the reference gas turbine (16.8 MW). A parametric study was carried out on the rich-zone equivalence ratio of the RQL combustor and on the fuel blend composition. The

goal was to identify the optimal design configuration of the new combustor, minimizing emissions while maintaining good performance.

As shown in Figure 4, NO_X emissions are strongly affected by both the equivalence ratio and the hydrogen fraction in the fuel blend, since these parameters directly influence flame temperature and radical concentrations. According to previous studies on NH_3/H_2 staged combustion [16], NO_X emissions in NH_3/H_2 rich–lean combustors are governed by the interaction between fuel-NO_X and thermal-NO_X mechanisms and by the different roles of the rich and lean combustion stages. When burning ammonia, NO_X formation is mainly associated with the fuel-NO_X pathway. Under fuel-rich conditions, however, the reducing environment promotes NO reduction through reactions with NH_i radicals, limiting the net NO_X formation in the rich stage. As the ϕ_r increases, the amount of unburned NH_3 leaving the rich stage increases. When this residual ammonia enters the lean stage, it is rapidly oxidized and converted to NO_X under lean conditions. Hydrogen addiction influences these mechanisms in two opposite ways. On one hand, hydrogen increases flame temperature and H-radical concentration, which can enhance thermal NO_X formation in the rich stage. On the other hand, increasing the hydrogen fraction reduces the ammonia content in the fuel mixture and promotes NH_3 decomposition in the rich stage. This significantly decreases the amount of unburned NH_3 entering the lean stage, thereby reducing lean fuel NO_X formation. For this reason, the effect of H_2 addition on resulting NO_X differs for low and high ϕ_r. At low ϕ_r, the increase in thermal NO_X due to H_2 addition outweighs the decrease in fuel NO_X. At high ϕ_r, however, the decrease in fuel NO_X due to H_2 addition exceeds the increase in thermal NO_X. As a matter of fact, H_2 addition compensates for the increase of NH_3 when increasing ϕ_r [16].

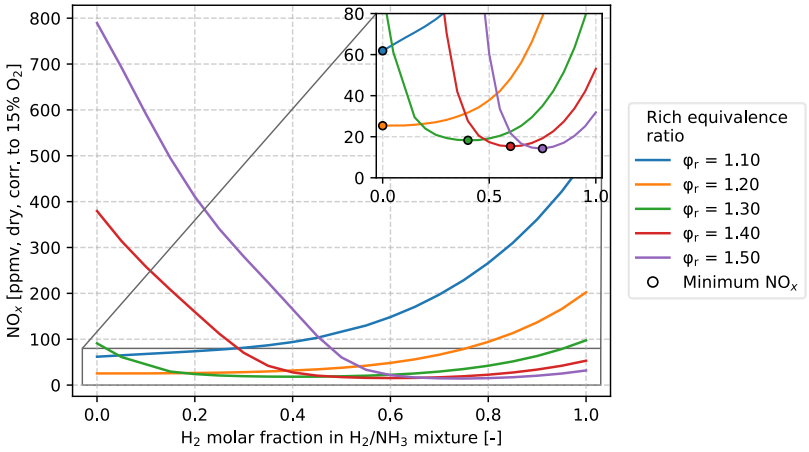

Figure 4: *NO_X emissions of the retrofitted gas turbine as a function of ϕ_r and fuel blend compositions.*

Figure 5 shows the effect of fuel composition and ϕ_r on the main performance parameters of the retrofitted gas turbine. The ϕ_r has a limited influence on the overall gas turbine performance. Noticeable differences appear only in cycle efficiency for high ammonia fractions and rich equivalence ratios of 1.4-1.5. Under these conditions a larger portion of ammonia remains unburned, which reduces the effective heat release. As a result, part of the chemical energy is not converted into useful work and the cycle efficiency decreases.

Changing the fuel composition primarily affects the mass flow rates across the turbine components. Fuels with a lower LHV require a higher fuel mass flow rate to meet the same power demand, although the exact thermal input may vary due to changes in cycle efficiency. This results in an increase in the total mass flow through the turbine as the ammonia fraction rises. The larger exhaust mass flow alters the turbine work balance. At fixed low-pressure shaft speed, the same power can be delivered with a smaller specific enthalpy drop, which leads to a lower TIT. This explains the reduction in the specific enthalpy drops across both the High Pressure (HP) and Low Pressure (LP) turbines observed as the ammonia fraction increases, as shown in Figure 5.

Fuel composition also influences the thermodynamic properties of the combustion products. At the same equivalence ratio, ammonia combustion produces a larger fraction of nitrogen and a lower water vapor content compared with hydrogen combustion. However, ammonia also results in significantly lower flame temperatures. To reach the required turbine TIT, the amount of dilution air must therefore be reduced increasing ϕ_g, even though the target TIT remains lower for ammonia-rich mixtures. The reduction in excess air and the relatively larger contribution of combustion products slightly increase R and c_p of the combustion products,

despite the lower temperature. Figure 5 reports these two quantities, but their combined effect also leads to a slight increase in γ and R/γ as the ammonia fraction increases. This also contributes to allowing the turbine to generate the required power with a smaller temperature drop. As a further indication of this effect, if a higher TIT were imposed, ammonia-rich blends combustion would require an even higher ϕ_g to reach such temperature. This would further reduce the dilution air fraction in the combustion products, increasing the c_p of the working fluid. In this case, the higher c_p would also contribute to the turbine power, reinforcing the tendency toward lower TIT in ammonia-rich mixtures.

These changes shift the operating equilibrium of the turbomachinery. To interpret how the operating points move on the compressor and turbine maps, corrected quantities are introduced. In particular, the corrected mass flow rate and corrected rotational speed are defined as [22]:

$$\dot{m}_{corr} = \left(\dot{m}\frac{\sqrt{RT}}{p\sqrt{\gamma}}\right)_{in} \tag{2}$$

$$N_{corr} = \left(\frac{N}{\sqrt{\gamma RT}}\right)_{in} \tag{3}$$

The LP turbine, with fixed rotational speed and geometry, is forced to operate at a slightly higher inlet pressure for high ammonia fractions due to the increased mass flow that must pass through the turbine section. Since the outlet pressure is fixed, the LP turbine expansion ratio increases. On the turbine map shown in Figure 6, higher ammonia fractions correspond to slightly lower corrected mass flow rates, because the decrease in inlet temperature and the rise in inlet pressure dominate the corrected flow definition, even though the actual mass flow rate and R/γ increase. The corrected speed line also increases due to the reduction in inlet temperature at constant rotational speed even if $R\gamma$ increase a bit. The compressor and HP turbine adjust to satisfy the HP shaft power balance. For increasing ammonia fractions, the HP turbine maintain almost the same expansion ratio, and the compressor operating conditions shift toward a higher pressure ratio driven by the LP turbine behavior. For constant thermal power as first approximation of constant shaft power output, the required air mass flow rate can be estimated from the AFR and the fuel LHV:

$$\dot{m}_{air,comb} = \dot{Q}\,\frac{AFR}{LHV} \tag{4}$$

Considering the resulting global equivalence ratios (ϕ_g ~ 0.29 for H_2 and ϕ_g ~ 0.33 for NH_3), both fuels yield very similar AFR/LHV ratio. As a result, nearly the same air mass flow rate is required to supply the same thermal power. At higher ammonia fractions the cycle operates at a slightly higher pressure ratio and γ, which leads to an increase in cycle efficiency:

$$\eta = 1 - \frac{1}{1-\beta^{(\gamma-1)/\gamma}} \tag{5}$$

As a result, less thermal power is required to produce the same shaft power, and the combustion air mass flow slightly decreases. The off-design HP turbine cooling flow remains nearly constant, as it is governed by pressure levels that change only marginally. Consequently, the total air mass flow rate decreases at higher ammonia fractions. The higher pressure ratio, but lower air mass flow rate results in lower HP spool velocity for increasing ammonia content. The HP turbine corrected mass flow decreases due to the combined effect of higher inlet pressure, lower inlet temperature despite higher mass flow rate and R/γ; the HP turbine corrected speed raises since the reduced TIT at denominator prevails (Figure 6).

A comparison between the methane design case and operation with NH_3/H_2 blends shows that the crossover in fuel mass flow occurs when the hydrogen molar fraction slightly exceeds 0.75. This corresponds to the composition at which the blend reaches the same LHV as methane. Despite this, when NH_3/H_2 mixtures are used, the turbine operates at a lower TIT than in the methane-fired baseline case. This behavior is mainly due to the higher c_p of the combustion products in the NH_3/H_2 case, largely associated with the higher H_2O content, which allows the turbine to generate the same power at lower temperature levels. This also contributes to the higher efficiency observed for NH_3/H_2 blends compared with methane, partly due to the higher value of γ (Eq. 5). The pressure ratio using the NH_3/H_2 blend becomes higher respect to the baseline methane case when the hydrogen fraction exceeds about 0.75, since the air mass flow rate is larger than in the methane case. Conversely, when the exhaust mass flow rate is lower than that of the baseline methane turbine, the resulting pressure ratio decreases.

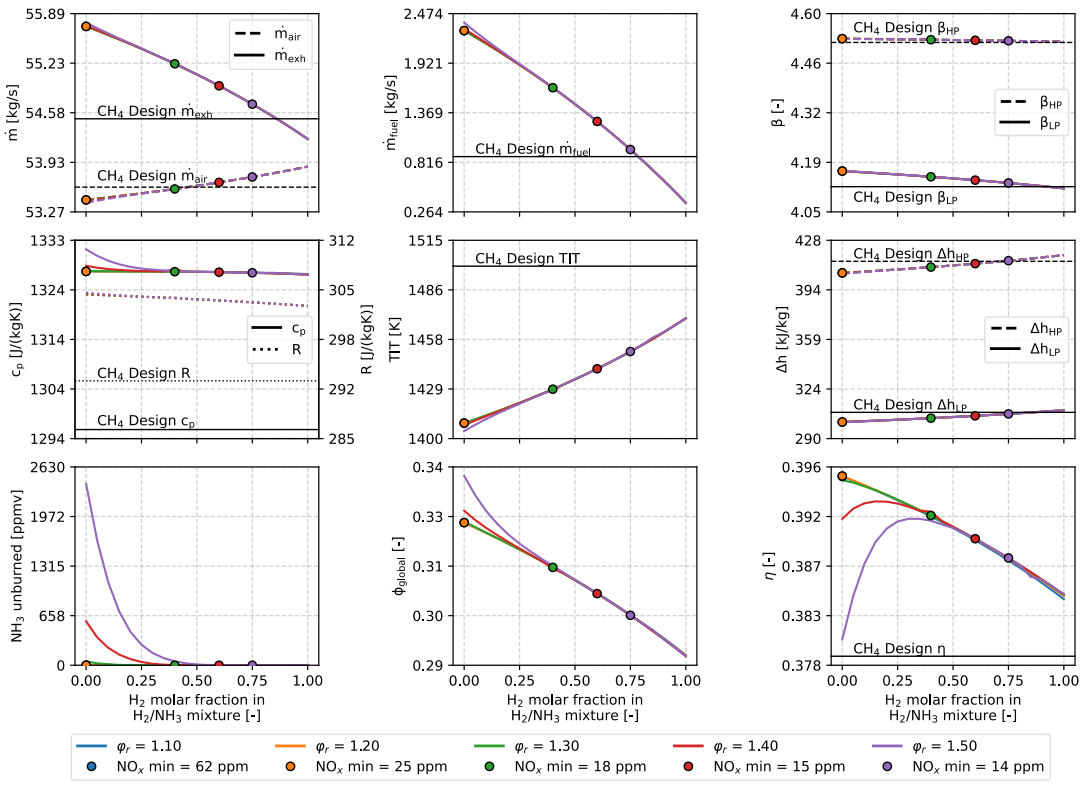

***Figure 5**: Performance trends of the retrofitted gas turbine (fixed power strategy) for different ϕ_r and fuel blend compositions. Solid and dashed horizontal lines indicate the reference baseline methane-fired design values. For each value of ϕ_r, the fuel blend corresponding to minimum NOx emissions is highlighted with a marker, and the associated minimum NOx value is reported in the legend.*

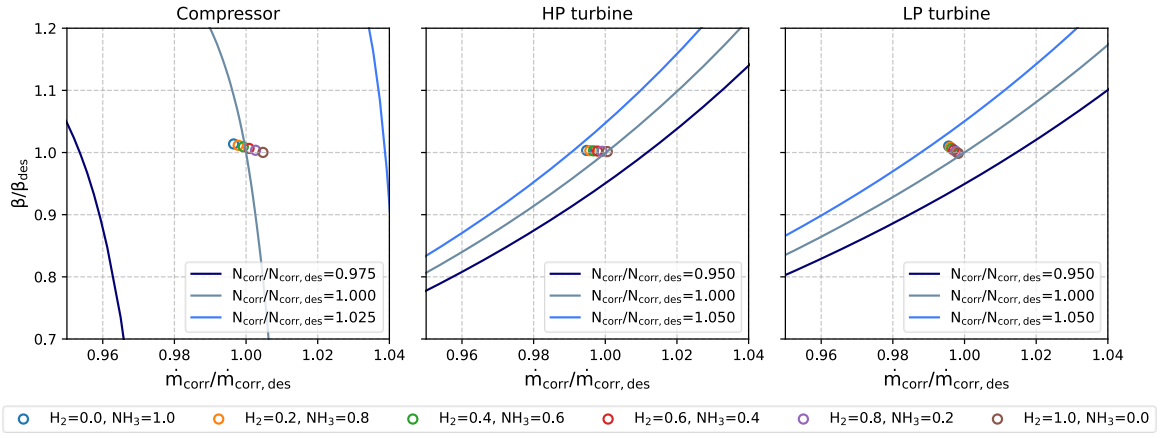

***Figure 6**: Performance maps of the compressor, HP turbine, LP turbine in corrected coordinates, showing operating points under retrofitting conditions for different fuel blends (molar fractions).*

The most balanced operating conditions are found at ϕ_r of 1.2 and 1.3, with H_2 molar fractions of 0% and 40%, respectively. In these conditions, NOx emissions are about 25 ppm and 18 ppm, respectively, while performance improves with increasing ammonia content. Further increasing the ϕ_r does not lead to a meaningful reduction in NOx emissions and requires higher hydrogen fractions. This would imply more extensive ammonia cracking, increasing system complexity while also penalizing cycle efficiency.

3.2.2 Maximum Power Retrofitting

To assess the full potential of the new fuel blends, the gas turbine can also be retrofitted to operate at its maximum achievable power. Since emissions mainly depend on ϕ_r, which is a combustor design parameter, the trend reported in Figure 4 remains remains unchanged. In fact, the low-NOx region is not affected by ϕ_g, which instead differs between the two retrofitting strategies since the TIT changes. As a result, the minimum NOx levels remain essentially the same across operating conditions. As already observed for the fixed power

retrofitting strategy, performance is largely insensitive to ϕ_r, except at high ϕ_r values combined with high ammonia fractions. This operating region is not of practical interest due to the associated high NO_X emissions and unburned NH_3. For this reason, the analysis is carried out at a fixed $\phi_r = 1.3$, varying only the fuel composition. The same trends apply to other ϕ_r values outside the aforementioned non-relevant region. When operating at maximum power for each fuel blend, two main constraints are imposed. The TIT is limited to the value of the baseline methane-fueled gas turbine, and the rotational speed of the high-pressure spool is capped at 105% of the nominal design speed, that is the manufacturer's maximum allowable limit [18].

The variation in maximum achievable power with fuel composition is primarily governed by which constraint becomes active. Beyond a hydrogen content of ~0.75, the TIT limit is reached before the rotational speed limit, as shown in Figure 7. This occurs because hydrogen-enriched fuels require a lower fuel mass flow while maintaining nearly the same air mass flow for a given thermal input, and they lead to higher TIT. As a result, when the thermal input is increased to boost power output, the thermal limit is reached earlier as the hydrogen fraction rises. In the thermal-limited regime, further increases in hydrogen content reduce the total energy input to the cycle, since the fuel mass flow decreases and the TIT is fixed. Consequently, air mass flow rate and exhaust gas mass flow rate decrease. At the same time, the lower exhaust mass flow requires a reduced expansion ratio in the LP turbine, which leads to a decrease in both the overall pressure ratio and the specific enthalpy drop. The combined reduction in exhaust mass flow and specific work results in a net decrease in maximum achievable power. In the rpm-limited regime, the HP spool speed is fixed, leading to an approximately constant air mass flow rate. The pressure ratio adjusts to match the LP turbine expansion requirements. The compressor work and corresponding HP turbine work are therefore fixed, and the fuel flow and the TIT adjusts accordingly to satisfy the required energy balance. For ammonia-rich mixtures, the higher fuel mass flow results in a larger exhaust mass flow, requiring a lower TIT and higher expansion ratio. As the hydrogen fraction increases, the fuel mass flow decreases, reducing the total mass flow and the expansion ratio through the turbine. Although for higher hydrogen fractions TIT increases, the associated rise in specific enthalpy drop is not sufficient to offset the reduction in exhaust mass flow, since the lower expansion ratio and c_p limit the achievable work. Also in this regime, the power output decreases with increasing hydrogen content.

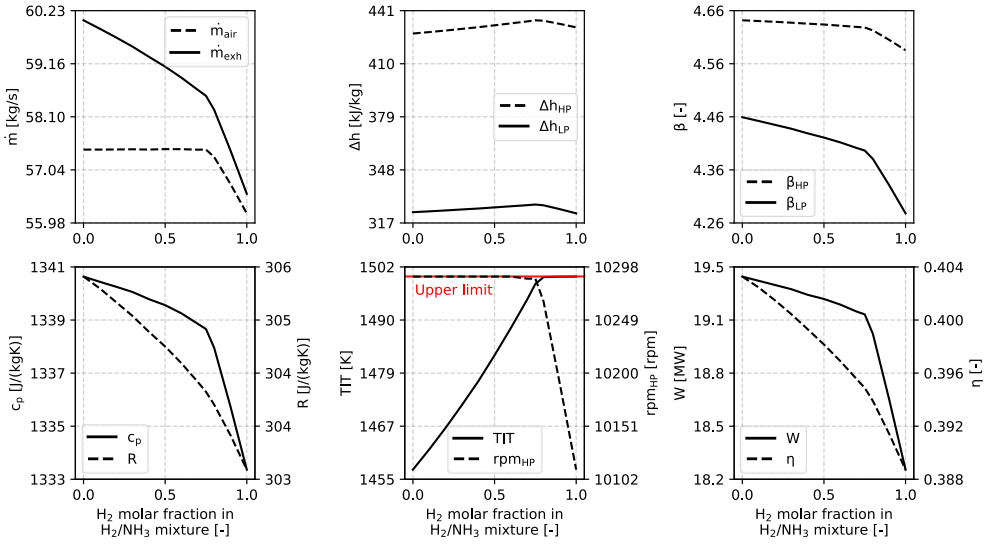

***Figure 7**: Performance trends of the retrofitted gas turbine (maximum power strategy) for $\phi_r = 1.3$ and different fuel blend compositions.*

When jointly considering maximum power output, efficiency, and emissions, ammonia-rich blends emerge as the most favorable option. Consistent with the fixed power retrofitting strategy, operating at ϕ_r 1.2 and 1.3 with ammonia fractions of 0% and 40% respectively provides the best compromise, ensuring higher power output and improved efficiency while maintaining low NO_X emissions and reducing the required cracking ratio.

4 Conclusions

This work assessed the retrofitting of a methane-fired gas turbine to NH_3/H_2 operation by modifying only the combustor while preserving the original turbomachinery. The analysis was carried out through a coupled

framework integrating a gas turbine cycle model with a detailed chemical reactor network for combustion modeling.

Fuel composition and rich-stage equivalence ratio were analyzed as the key parameters affecting NO_X emissions and performance. Two retrofitting strategies were investigated. In the low-NO_X region, which is the only one of practical interest for design, emissions for different fuel mixtures are strongly governed by the rich equivalence ratio, while performance is largely insensitive to it. This allows the rich equivalence ratio to be tuned to achieve low emissions without significantly affecting cycle performance, except at very high values combined with high ammonia fractions, where unburned NH_3 becomes relevant. As a result, once a low- NO_X operating region is identified, the corresponding emission behavior remains valid across different retrofitting strategies, while performance differences are driven by the strategy itself and by the fuel composition. In the fixed power strategy, the turbine delivers the same nominal output as the baseline configuration, making it suitable for existing plants. Under these conditions, ammonia-rich mixtures slightly improve efficiency, while lower hydrogen fractions are beneficial to limit the energy and complexity associated with ammonia cracking. In the maximum power strategy, the turbine operates at its maximum achievable output within thermal and mechanical constraints. The limiting factor is either turbine inlet temperature or rotational speed, depending on the fuel blend. Also in this case, ammonia-rich mixtures are more advantageous, as they allow higher power output and maintain higher efficiency. From this perspective, operating with high ammonia fractions is beneficial from a performance standpoint. Since low NO_X emissions can still be achieved by properly selecting the rich equivalence ratio, even with limited hydrogen content, the best trade-off is obtained for rich equivalence ratios of 1.2–1.3 and moderate hydrogen fractions of 0 and 40% respectively. These conditions enable NO_x emissions around 20 ppm while maintaining performance levels closer to ammonia-rich operation, which are more favorable than those obtained with high hydrogen content.

Overall, the proposed framework supports both combustor design choices and retrofitting strategy selection. Properly optimized NH_3/H_2 mixtures, combined with suitable staged combustion design, can enable efficient and low-emission carbon-free power generation. The preferred strategy depends on whether the priority is operational continuity or maximum performance.

Nomenclature

Acronyms

AFR	Air-Fuel Ratio
CRN	Chemical Reactor Network
DLN	Dry Low NOx
HP	High Pressure
LHV	Lower Heating Value
LP	Low Pressure
PFR	Plug Flow Reactor
PSR	Perfectly Stirred Rector
RQL	Rich-burn/Quick-mix/Lean-burn
TIT	Turbine Inlet Temperature

Symbols

c_p	Specific heat capacity at constant pressure
h	Specific enthalpy
$\dot{m}$	Mass flow rate
N	Rotational speed
p	Pressure
$\dot{Q}$	Thermal power
R	Gas constant
W	Power

Subscripts and superscripts

air	Air
$corr$	Corrected
$comb$	Combustion
exh	Exhaust
$fuel$	Fuel
in	Inlet
nom	Nominal
r	Rich
g	Global

Greek Symbols

β	Pressure ratio
γ	Heat capacity ratio
Δ	Difference
η	Efficiency
ϕ	Equivalence ratio

Acknowledgments

This work was supported by the European Union's HORIZON EUROPE Research and Innovation Programme under grant agreement no. 101137625 (ACHIEVE).

References

[1] Sun J, Zhao N, Zheng H. A comprehensive review of ammonia combustion: Fundamental characteristics, chemical kinetics, and applications in energy systems. Fuel 2025;394.

[2] Saif AGH, Mokheimer EMA. Comprehensive review on ammonia combustion technologies: Combustion characteristics, potential of hydrogen/methane additions, and emerging applications. Int J Hydrogen Energy 2025;148.

[3] Yao N, Pan W, Zhang J, Wei L. The advancement on carbon-free ammonia fuels for gas turbine: A review. Energy Convers Manag 2024;315.

[4] Carcasci C, Facchini B. A numerical method for power plant simulations. Journal of Energy Resources Technology, Transactions of the ASME 1996;118:36–43.

[5] Andreini A, Facchini B. Gas turbines design and off-design performance analysis with emissions evaluation. J Eng Gas Turbine Power 2004;126:83–91.

[6] Gamannossi A, Bertini D, Adolfo D, Carcasci C. Analysis of the GT26 single-shaft gas turbine performance and emissions. Energy Procedia, vol. 126, Elsevier; 2017, p. 461–8.

[7] Zhou J, Duan F. Combustion and emission characteristics of industrial gas turbine combustor fueled with partially cracked ammonia: Effects of fuel–air staging and mixing. J Clean Prod 2025;521:146205.

[8] Li Z, Li S. Effects of inter-stage mixing on the NOx emission of staged ammonia combustion. Int J Hydrogen Energy 2022;47:9791–9.

[9] Li Z, Zhang Y, Zhang H. Kinetics modeling of NOx emission of oxygen-enriched and rich-lean-staged ammonia combustion under gas turbine conditions. Fuel 2024;355.

[10] Rocha RC, Costa M, Bai XS. Combustion and Emission Characteristics of Ammonia under Conditions Relevant to Modern Gas Turbines. Combustion Science and Technology 2021;193:2514–33.

[11] Bedick C, Boyette W. Chemical Reactor Network Modeling of Ammonia Rich-Quench-Lean Combustion Using a Partially Stirred Reactor Approach. Proceedings of the ASME Turbo Expo, vol. 3A-2025, American Society of Mechanical Engineers Digital Collection; 2025. https://doi.org/10.1115/GT2025-152893.

[12] Goodwin DG, Moffat HK, Schoegl I, Speth RL, Weber BW. Cantera: An Object-Oriented Software Toolkit for Chemical Kinetics, Thermodynamics, and Transport Processes 2025. http://www.cantera.org.

[13] Orbegoso EMM, Romeiro CD, Ferreira SB, Da Silva LFF. Emissions and thermodynamic performance simulation of an industrial gas turbine. J Propuls Power 2011;27:78–93.

[14] Smith GP, Golden DM, Frenklach M, Moriarty NW, Eiteneer B, Goldenberg M, et al. GRI-MECH 3.0 2025. http://www.me.berkeley.edu/gri_mech/.

[15] Egawa T, Hayashi A, Sato K, Nagashi H, Fukuba S, Nakamura S. Hydrogen/Ammonia-fired Gas Turbine Initiatives for Carbon Neutrality. vol. 60. 2023.

[16] Li Z, Li S. Kinetics modeling of NOx emissions characteristics of a NH3/H2 fueled gas turbine combustor. Int J Hydrogen Energy 2021;46:4526–37.

[17] Okafor EC, Naito Y, Colson S, Ichikawa A, Kudo T, Hayakawa A, et al. Experimental and numerical study of the laminar burning velocity of CH4–NH3–air premixed flames. Combust Flame 2018;187:185–98.

[18] Asti A, Gamberi F, Del Vescovo G, Carta R, Giannini N, Ignesti M, et al. Heavy Duty Gas Turbine Performance and Endurance Testing: The NovaLT^{TM}16 Experience 2018.

[19] Taylor M. HP Turbine Aerodynamic Design Insights. VKI Lecture Series. 2006.

[20] Hall DK, Greitzer EM, Tan CS. Performance limits of axial compressor stages. Proceedings of the ASME Turbo Expo, vol. 8, American Society of Mechanical Engineers Digital Collection; 2012, p. 479–89.

[21] Sanaye S, Hosseini S. Off-design performance improvement of twin-shaft gas turbine by variable geometry turbine and compressor besides fuel control. Proceedings of the Institution of Mechanical Engineers, Part A: Journal of Power and Energy 2020;234:957–80.

[22] Kim SR, Jeong JH, Kim TS. Investigation of operational strategies of natural gas-hydrogen-ammonia co-fired gas turbine combined cycle in simultaneous consideration of performance and CO2 emission. Case Studies in Thermal Engineering 2025;73:106584.